Supporting Information

Sandwich double-decker Er(III) and Yb(III) complexes, containing naphthalocyanine moiety: synthesis and investigation of effect of a paramagnetic metal center

Tatiana V. Dubinina,[a,b] Elizaveta F. Petrusevich,[a] Anton D. Kosov,[a] Nataliya E. Borisova,[a,c] Alexander L. Trigub,[d] George V. Mamin,[e] Ildar F. Gilmutdinov,[e] Artem A. Masitov,[f] Sergey V. Tokarev,[f] Victor E. Pushkarev[b] and Larisa G. Tomilova[a,b]

[a.] *Chemistry Department, M.V. Lomonosov Moscow State University, 1 Leninskie Gory, 119991 Moscow, Russian Federation. Fax: +7 495 939 0290; E-mail: dubinina.t.vid@gmail.com*
[b.] *Institute of Physiologically Active Compounds, Russian Academy of Sciences, 1 Severny proezd, 142432 Chernogolovka, Moscow Region, Russian Federation*
[c.] *N.A. Nesmeyanov Institute of Organoelement Compounds, 28 Vavilov Str. 119334 Moscow, Russian Federation*
[d.] *National Research Center "Kurchatov Institute", pl. Akad. Kurchatova, dom 1, 123098 Moscow, Russia*
[e.] *Kazan Federal University, Institute of Physics, 18 Kremlyovskaya Str., 420008 Kazan, Russian Federation*
[f.] *Institute of Problems of Chemical Physics, Russian Academy of Sciences, 1 Academician Semenov avenue, 142432 Chernogolovka, Moscow Region, Russian Federation*

Contents list

Fig. S19. Thermogram (A) and results of evolved gas analysis by mass-spectrometry (B) for complex **4b**.

Table S1. High-resolution mass spectrometry MALDI TOF/TOF data.

Compound (Molecular formula)	Mass found	Monoisotopic mass calculated
3a ($C_{128}H_{73}ErN_{16}$)	1999.8943	1999.5507
3b($C_{128}H_{73}N_{16}Yb$)	2007.2751	2007.5593
3c($C_{128}H_{73}ErN_{16}O_8$)	2127.7750	2127.5100
3d ($C_{176}H_{105}ErN_{16}O_{16}$)	2863.8754	2863.7197
4b ($C_{192}H_{113}N_{16}Yb$)	2815.8752	2815.8723

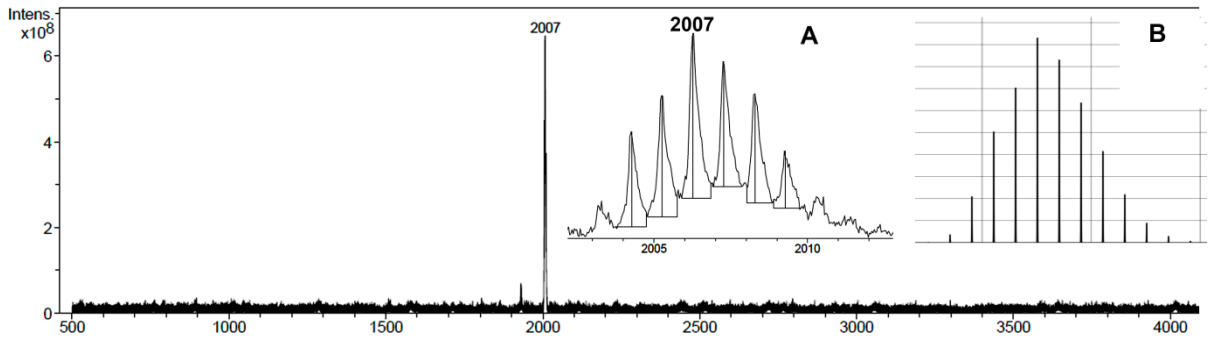

Fig. S1. MALDI-TOF mass spectrum of **3b**, isotopic pattern for the molecular ion (inset A) and simulated MS pattern of the molecular ion (inset B).

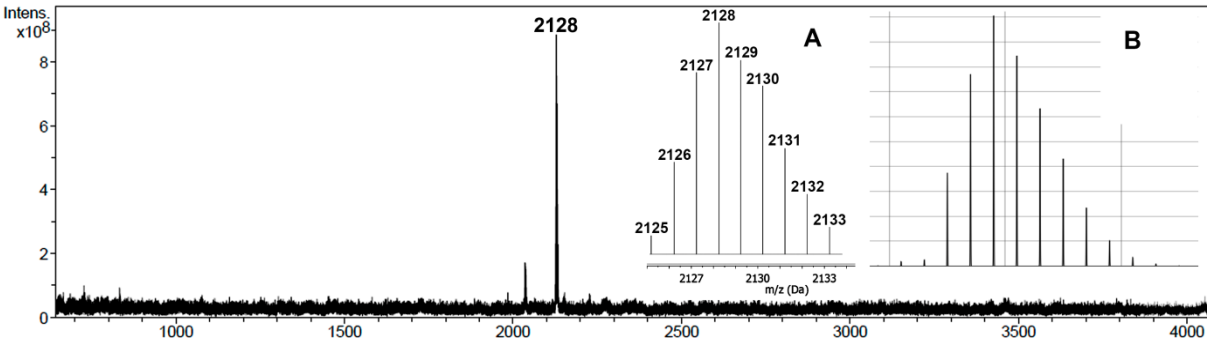

Fig. S2. MALDI-TOF mass spectrum of **3c**, isotopic patterns for the molecular ion (inset A) and simulated MS patterns of the molecular ion (inset B).

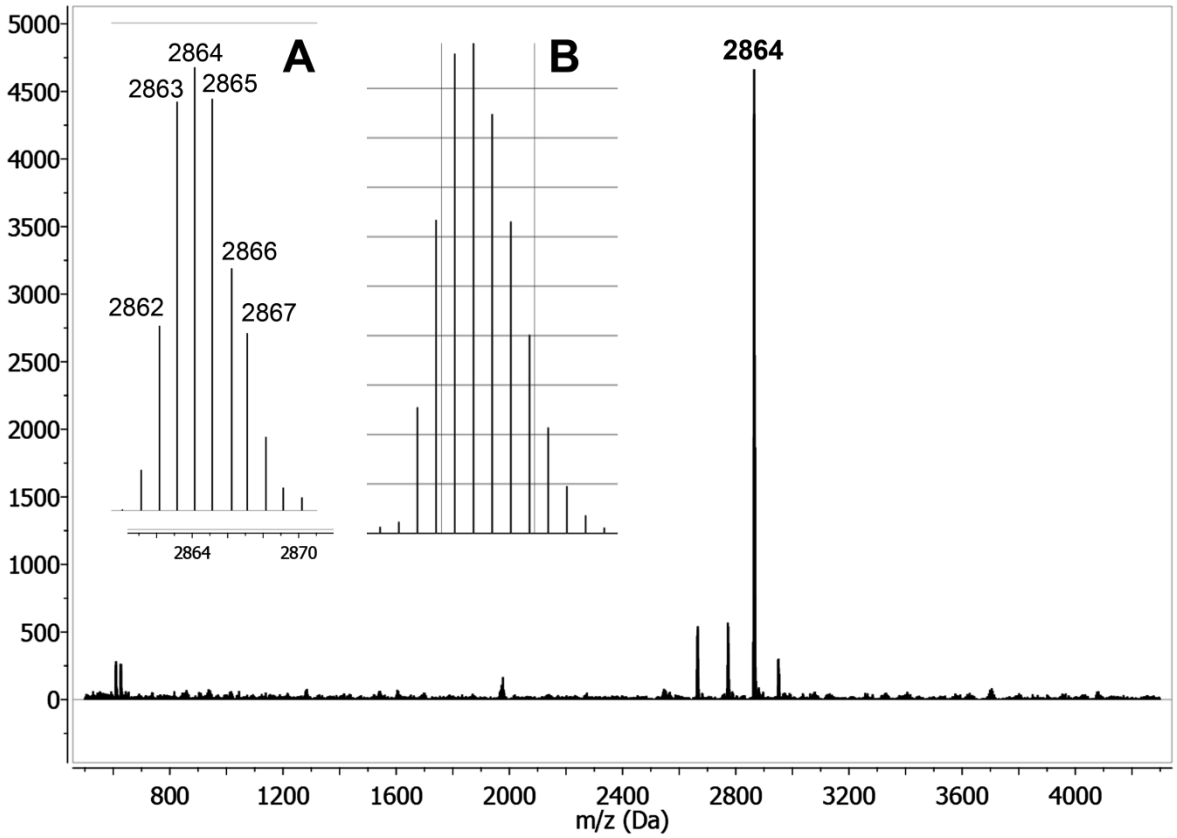

Fig. S3. MALDI-TOF mass spectrum of **3d**, isotopic patterns for the molecular ion (inset A) and simulated MS patterns of the molecular ion (inset B).

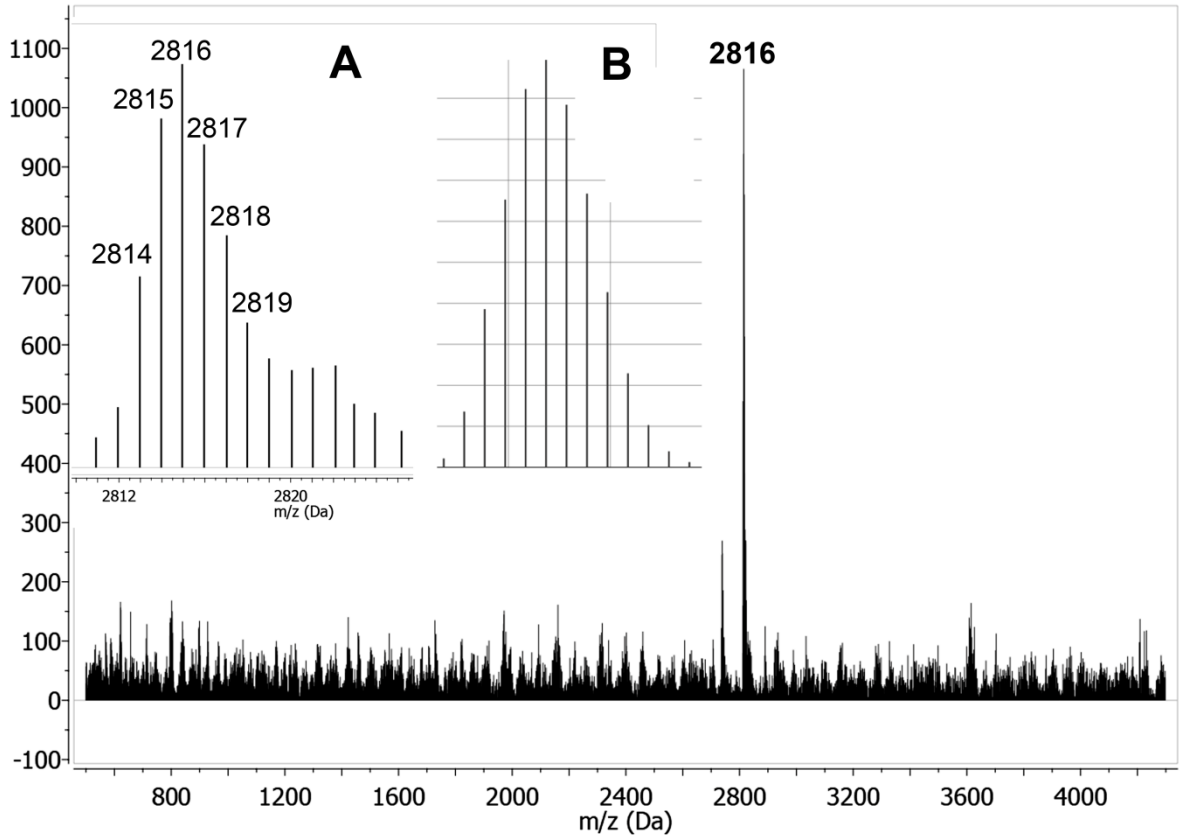

Fig. S4. MALDI-TOF mass spectrum of **4b**, isotopic patterns for the molecular ion (inset A) and simulated MS patterns of the molecular ion (inset B).

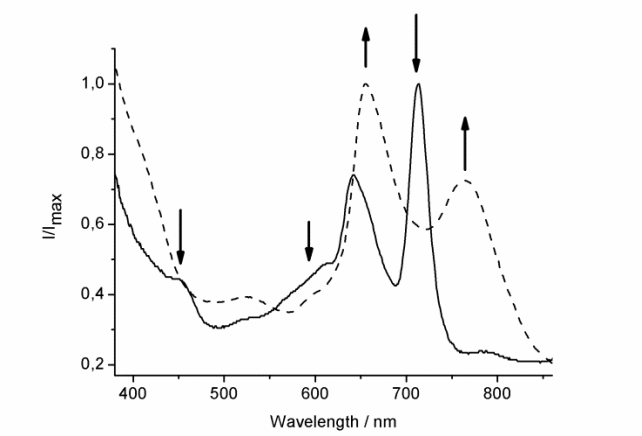

Fig. S5. Spectral changes during reduction of complex **3a** with $N_2H_4 \times H_2O$ in THF solution (solid line – initial forms, dashed lines – reduced form).

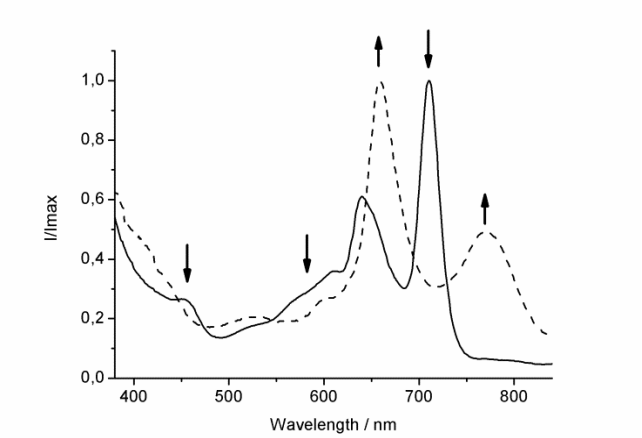

Fig. S6. Spectral changes during reduction of complex **3b** with $N_2H_4 \times H_2O$ in THF solution (solid line – initial forms, dashed lines – reduced form).

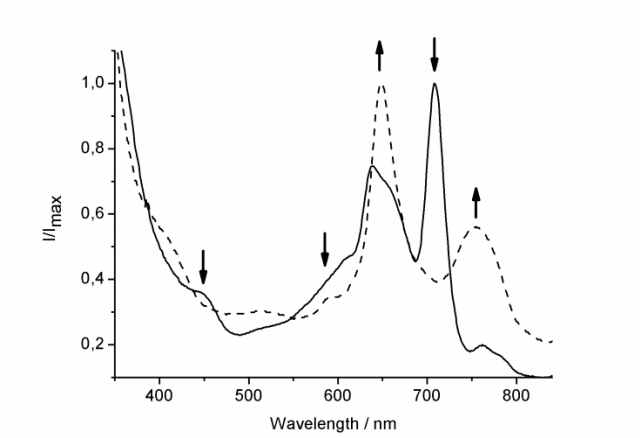

Fig. S7. Spectral changes during reduction of complex **3c** with $N_2H_4 \times H_2O$ in THF solution (solid line – initial forms, dashed lines – reduced form).

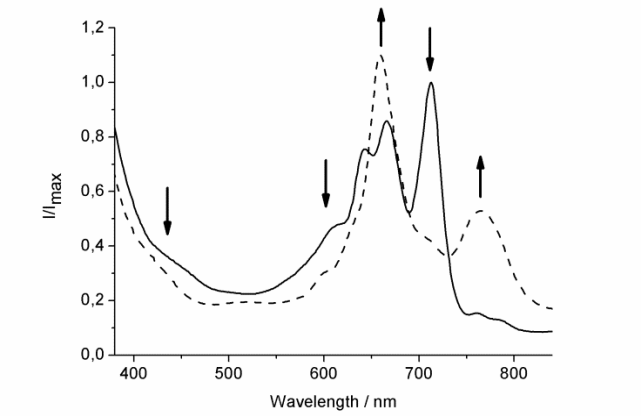

Fig. S8. Spectral changes during reduction of complex **3d** with $N_2H_4 \times H_2O$ in THF solution (solid line – initial forms, dashed lines – reduced form).

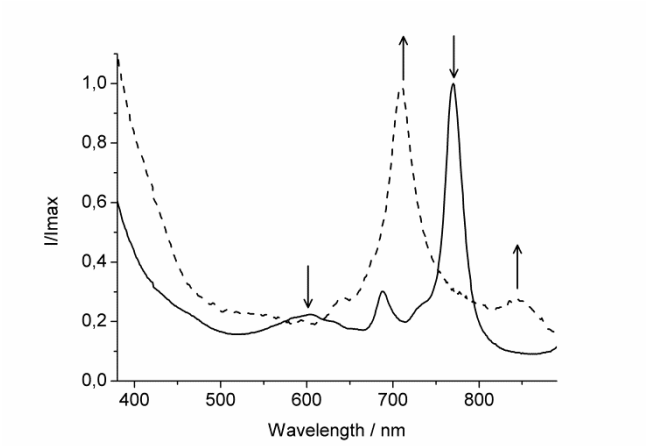

Fig. S9. Spectral changes during reduction of complex **4b** with $N_2H_4 \times H_2O$ in THF solution (solid line – initial forms, dashed lines – reduced form).

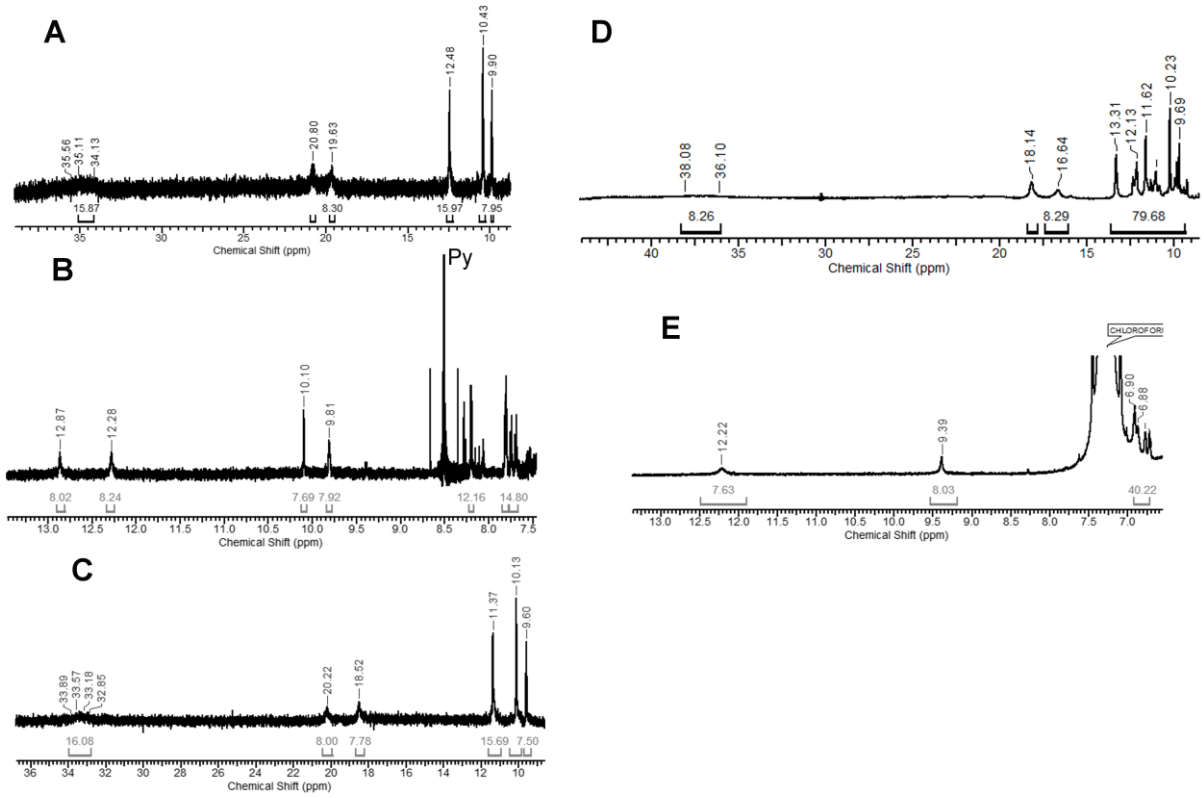

Fig. S10. ^{1}H NMR spectra of complexes **3a-d** (A-D respectively) and **4b** (E) in the presence of $N_2H_4 \times H_2O$.

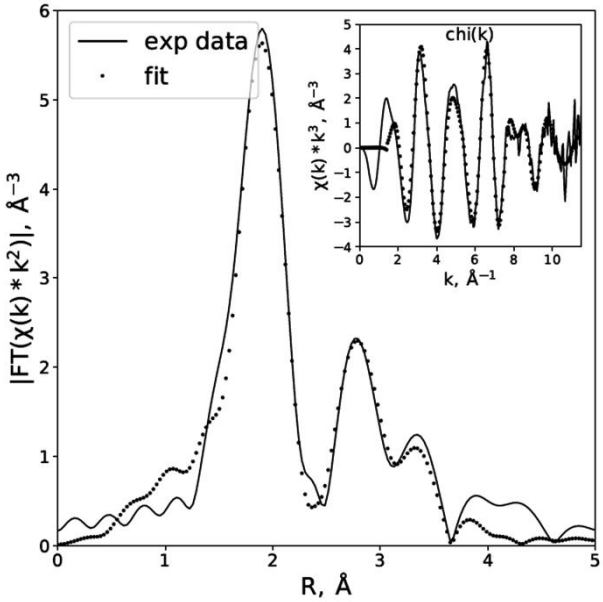

Fig. S11. Fitted EXAFS spectrum for **4b** in R- and k-spaces.

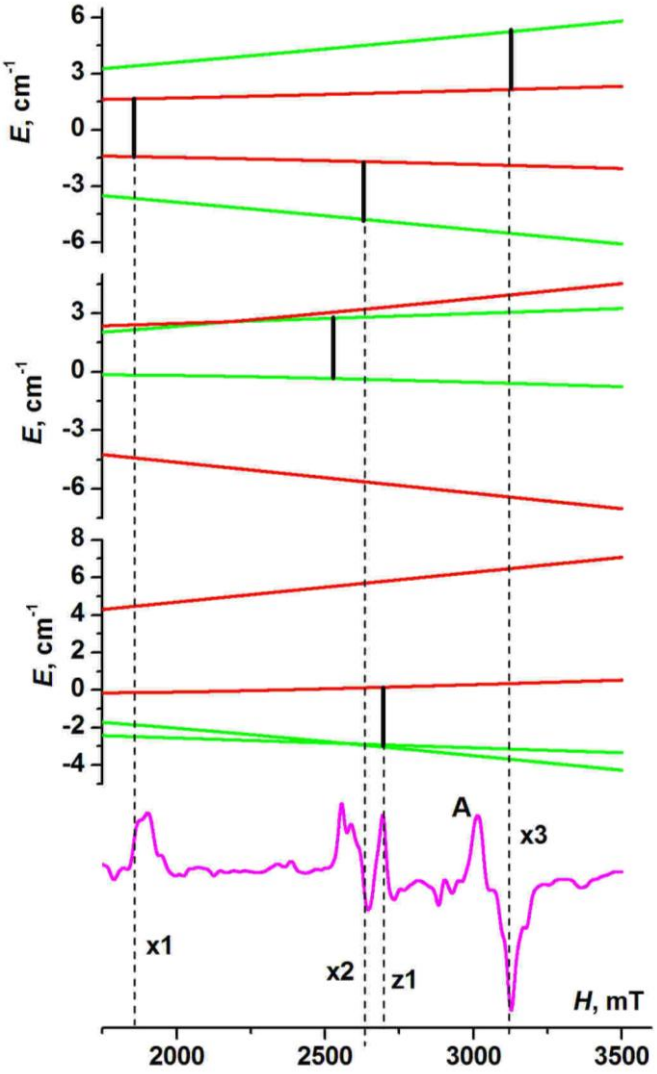

Fig. S12. Zeeman energy levels, allowed transitions, and theoretical ESR spectrum of Yb^{3+} ion in quartet state ($S = 3/2$) with zero-field slitting parameters $|D_{Yb}| = 1.46$ cm^{-1}, $E = 0.385$ cm^{-1}, $g_{iso\_Yb} = 2.34$. "A" denotes the "extra" line.

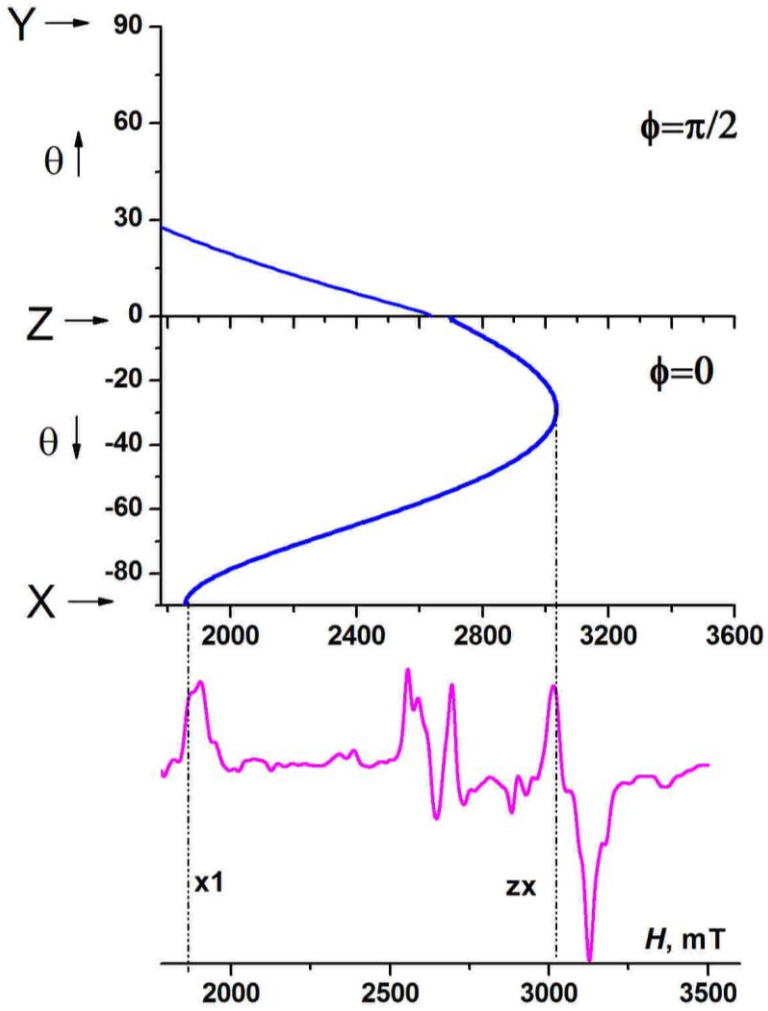

Fig. S13. Angular dependency diagram for the quartet state ($S = 3/2$) with zero-field splitting parameters $|D_{Yb}| = 1.46$ cm^{-1}, $E = 0.385$ cm^{-1}, $g_{iso\_Yb} = 2.34$.

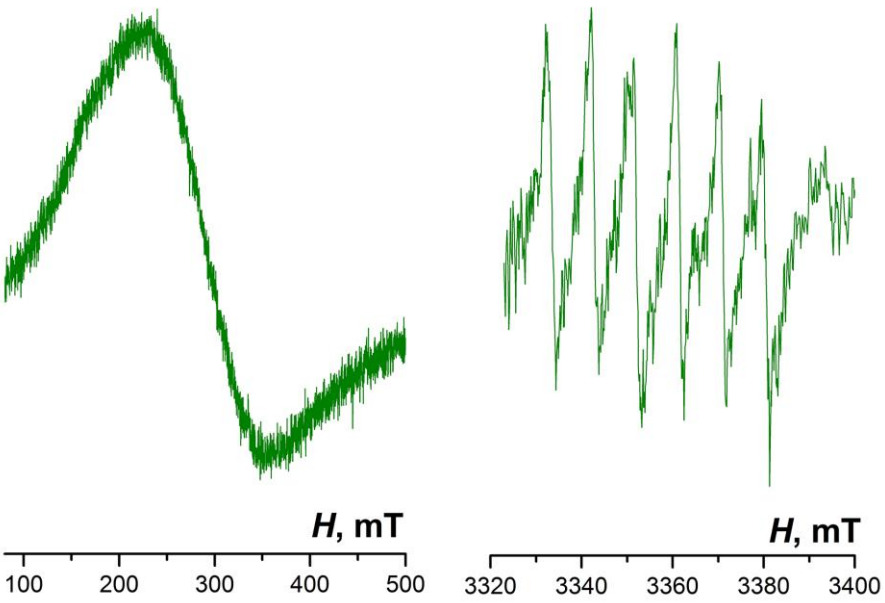

Fig. S14. A low-field (left) and a high-field (right) parts of the experimental W-band EPR spectrum of [**4b**]$^{-}$ in THF solution at T = 25 K. The low-field part reveals $g_{\perp}$ line, and the high-field part shows the hyperfine structure for Yb^{3+} ion (I_{Yb} = 5/2) with a constant of hyperfine interaction a_{Yb} = 10 mT.

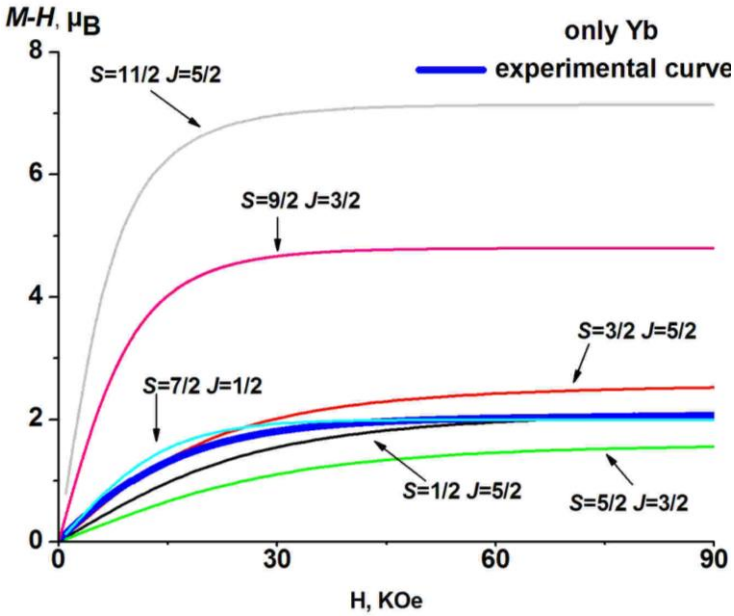

Fig. S15. Calculated *M-H* curves for Yb^{3+} ion (experimental curve is marked in blue).

Table S2. Magnetic parameters of calculated *M-H* curves (see Fig. S15) for Yb^{3+} ion without *f*-π interaction. For S_{Yb} = 1/2, 3/2, 5/2 and 7/2, the cases with $R \leq 2$ μ_B are given. For S_{Yb} = 9/2, 11/2 and 13/2, the cases with minimal *R* values are given.

S_{Yb}	L_{Yb}	J_{Yb}	R, μ_B
1/2	3	5/2	0.19
1/2	3	7/2	1.66
3/2	3	3/2	1.52
3/2	3	5/2	0.32
3/2	3	7/2	1.99
5/2	3	1/2	1.64
5/2	3	3/2	0.58
5/2	3	5/2	1.02
7/2	3	1/2	0.10
7/2	3	3/2	0.85
7/2	3	5/2	2.03
9/2	3	3/2	2.67
11/2	3	5/2	4.90
13/2	3	7/2	7.01

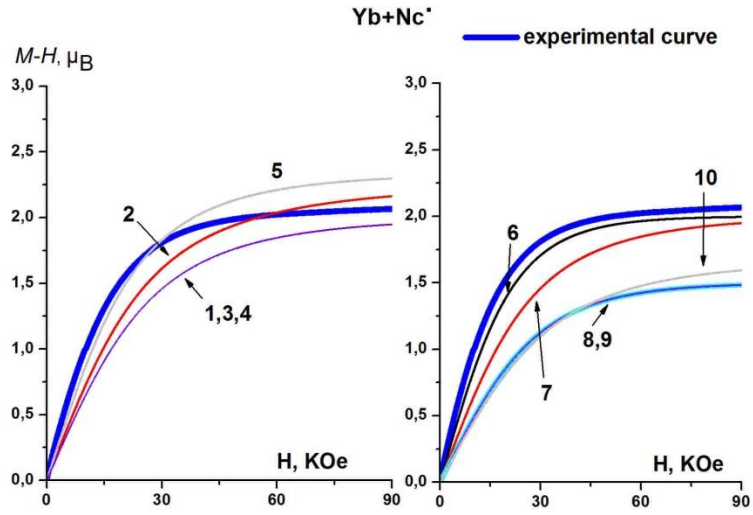

Fig. S16. Calculated *M-H* curves considering *f*-π interaction of Yb^{3+} and unpaired π-electron at the Nc-decks (curve numbers correspond to the numbers in Table S3).

Table S3. Magnetic parameters of calculated *M-H* curves (see Fig. S16) considering *f*-π interaction of the Yb^{3+} ion *f*-shell and the unpaired π-electron at the Nc-decks. In the cases of S_{Yb} = 7/2, 9/2, 11/2 and 13/2, the value of $R > 1.7\ \mu_B$.

Curve number	S_{Yb}	L_{Yb}	S_{Nc}	L_{Nc}	J_{total}	Interaction type	R, μ_B
1	1/2	3	1/2	1	2	Antiferro-	0.26
2	1/2	3	1/2	1	3	Ferro-	0.15
3	3/2	3	1/2	0	2	Antiferro-	0.90
4	3/2	3	1/2	0	2	Ferro-	0.26
5	3/2	3	1/2	1	2	Antiferro-	0.15
6	3/2	3	1/2	1	1	Ferro-	0.10
7	5/2	3	1/2	0	2	Antiferro-	0.26
8	5/2	3	1/2	0	1	Ferro-	0.60
9	5/2	3	1/2	1	3	Antiferro-	0.60
10	5/2	3	1/2	1	1	Ferro-	0.58

Table S4. Crystal field splitting parameters and spin-orbital coupling constant (λ) for **4b**, [**4b**]$^{-}$ and $[Pc_2Yb]^{-}TBA^{+}$.

Sample	Energy, cm^{-1}				λ, cm^{-1}
	$E_1 = E(l_z = -1) - E(l_z = 3)$	$E_2 = E(l_z = 3) - E(l_z = 2)$	$E_3 = E(l_z = 2) - E(l_z = 1)$	$E_4 = E(l_z = 1) - E(l_z = 0)$	
$[Pc_2Yb]^{-}TBA^{+}$	46	255	5	100	–126.5
[**4b**]$^{-}$	410	1355	80	1500	–68.5
4b	325	1355	70	1500	–57.2

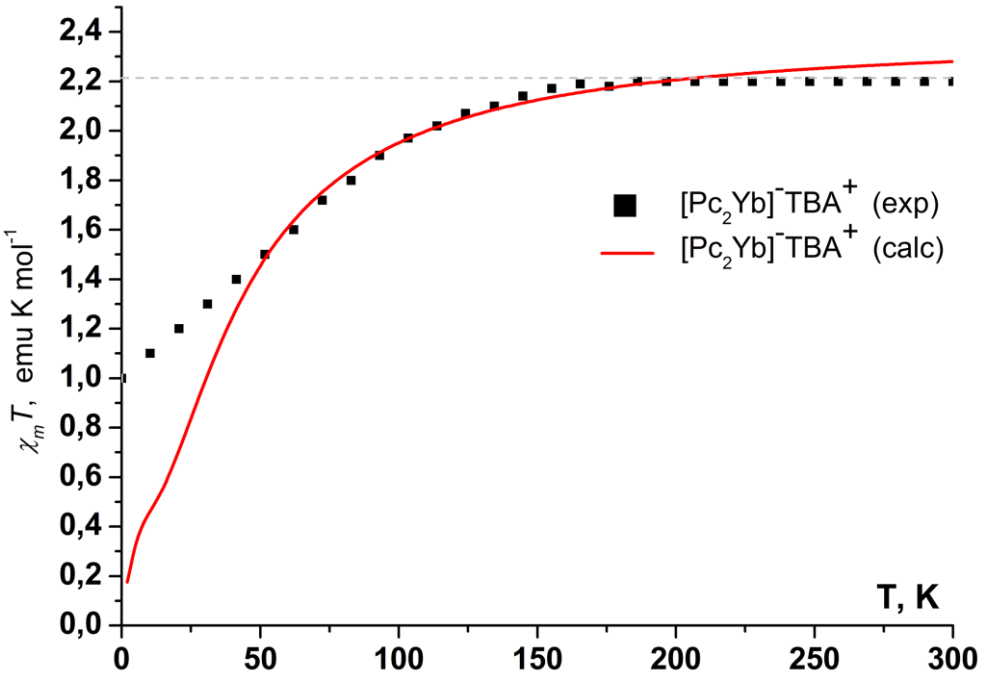

Fig. S17. Experimental and theoretical χ_mT curves for $[Pc_2Yb]^{-}TBA^{+}$. The experimental curve was reconstructed in the Origin 7.0 program according to the earlier published data.[36] The theoretical curve was obtained based on the Van Vleck equation using parameters given in Table S4 for the case (b), when $E_{crystal\ field} > E_{SOC}$.

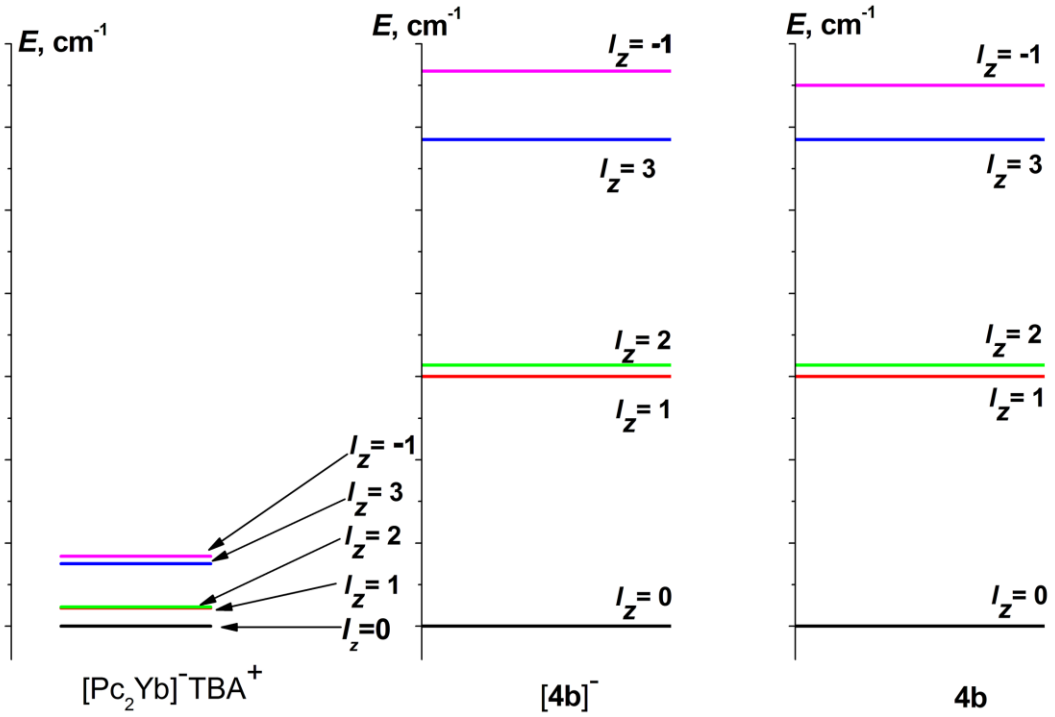

Fig. S18. Schematic representation of the crystal filed splitting for $[Pc_2Yb]^-TBA^+$, $[\mathbf{4b}]^-$ and **4b**. Sublevels marked with the same color have the same I_z value.

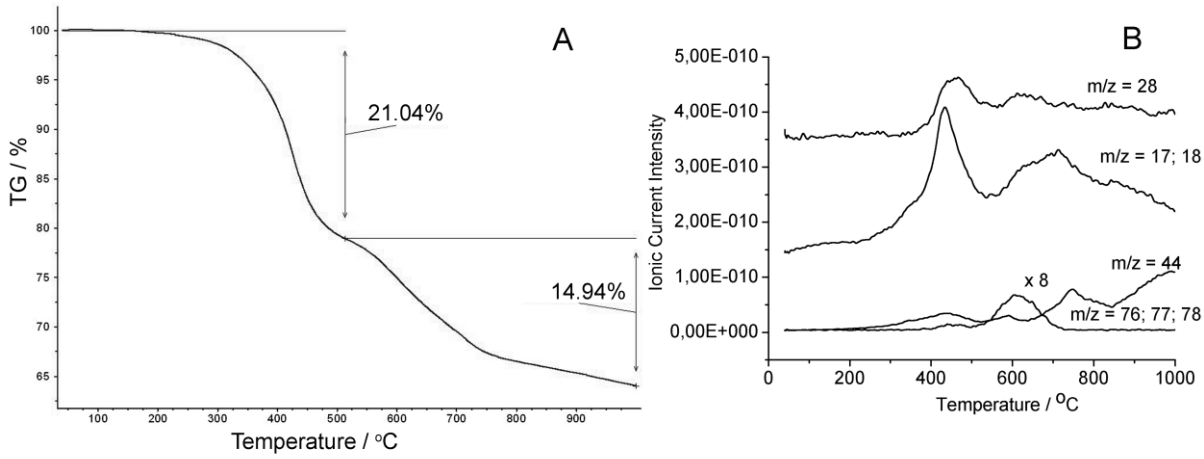

Fig. S19. Thermogram (A) and results of evolved gas analysis by mass-spectrometry (B) for complex **4b**.